

# Acute myocardial infarction: early CT aspects of myocardial microcirculation obstruction after percutaneous coronary intervention

Charles Amanieu · Ingrid Sanchez · Simona Arion ·  
Eric Bonnefoy · Didier Revel · Philippe Douek ·  
Loic Boussel

Received: 28 December 2012 / Revised: 28 February 2013 / Accepted: 1 March 2013 / Published online: 8 May 2013  
© European Society of Radiology 2013

## Abstract

**Objective** To evaluate the capabilities of delayed enhanced multidetector CT (DE-MDCT), performed immediately after percutaneous coronary intervention (PCI), in predicting myocardial microvascular obstruction (MVO) formation assessed by delayed enhanced MRI (DE-MRI).

**Methods** Thirty-two patients presenting with a primary acute myocardial infarction, successfully recanalised by PCI, underwent a DE-MDCT immediately after PCI and a DE-MRI within 1 week. The left ventricle was split into 64 subsegments, rated as “healthy”, “infarcted” or “MVO” on DE-MRI. Their mean density was measured on DE-MDCT and calculated relative to the patient’s mean healthy myocardium density. Hypoenhanced DE-MDCT subsegments, termed “CT early MVO”, were also recorded. Sensitivity and specificity of DE-MDCT for MRI-assessed “MVO” subsegments detection was calculated for mean CT relative

density (threshold determined from a ROC analysis), “CT early MVO” and both.

**Results** Mean CT relative density was higher in MRI-assessed “MVO” than in “infarcted” and “healthy” subsegments ( $1.82 \pm 0.46$ ,  $1.43 \pm 0.36$  and  $1.0 \pm 0.13$  respectively;  $P < 0.001$ ) leading to a sensitivity and specificity of 94.3 % and 89.2 % for a cutoff of 1.36. Sensitivity and specificity were respectively 16.9 % and 99.8 % for “CT early MVO” and 95.3 % and 89.3 % when considering the two patterns.

**Conclusion** DE-MDCT, performed immediately after PCI, allows for an accurate prediction of MVO formation.

## Key Points

- Myocardial microvascular obstruction (MVO) is an important prognostic sequel following myocardial infarction.
- MVO can be accurately predicted by multidetector CT (MDCT).
- Both hypo- and hyperenhanced myocardial areas can be analysed by MDCT.
- MDCT may become a useful prognostic tool for acute MI outcome.

C. Amanieu · I. Sanchez · S. Arion · D. Revel · P. Douek  
Department of Radiology, Louis Pradel Hospital, CREATIS,  
CNRS UMR 5220, INSERM U1044, Lyon, France

E. Bonnefoy  
Department of Cardiology, U51, Louis Pradel Hospital, Lyon,  
France

L. Boussel  
Department of Radiology, Croix-Rousse Hospital, CREATIS,  
CNRS UMR 5220, INSERM U1044, Lyon, France

L. Boussel (✉)  
Department of Radiology, Croix-Rousse Hospital, 103,  
Grande rue de la Croix-Rousse,  
69004 Lyon, France  
e-mail: loic.boussel@gmail.com

**Keywords** CT systems, X-Ray computed · Magnetic resonance imaging · Myocardial infarction · Myocardial microvascular obstruction · Delayed enhancement

## Abbreviations

DE-MDCT	Delayed enhanced multidetector CT
MVO	Myocardial microvascular obstruction
PCI	Percutaneous coronary intervention
DE-MRI	Delayed-enhanced magnetic resonance imaging
CK	Creatine kinase
MPR	Multiplanar reconstruction

## Introduction

Persistent myocardial microvascular obstruction (MVO), also termed as “no reflow”, is an important predictor of adverse outcome in patients after acute myocardial infarction [1–5]. It corresponds to myocardial microcirculation obstruction [6–8] resulting from three main mechanisms occurring successively in time: ischaemic injury during the coronary artery occlusion, distal atherothrombotic embolisation, mainly resulting from percutaneous coronary intervention (PCI), and ischaemia–reperfusion injury [9–11]. Early estimation of MVO, as well as assessment of infarct size, may help in establishing an accurate prognostic and adapt patients’ treatment in clinical practice. Post-gadolinium delayed-enhanced magnetic resonance imaging (DE-MRI) is a well-established non-invasive imaging technique that allows for MVO assessment [12] by studying the sparing of the immediate sub-endocardial myocardium by contrast enhancement in regions of myocardial infarction. However, the usefulness of this technique in the acute setting is limited because of the time required for the examination and difficulties in monitoring unstable patients inside the magnet.

Delayed enhanced multislice computed tomography (DE-MDCT) has been proposed to evaluate myocardial infarction during the acute phase, immediately after percutaneous coronary intervention (PCI) and without additional contrast agent injection [13, 14]. In a previous work [14] we demonstrated that CT allows MVO to be assessed as an area of myocardial hypoenhancement but tends to underestimate it in comparison with DE-MRI, the reference method [12]. We observed that this underestimation may be because future MVO areas present not as hypo- but as hyperenhancement on DE-MDCT. This could be due to acute major areas of oedema and to an hyperaemic transitory response after reperfusion of areas with later impaired tissue perfusion (i.e. MVO zones) [6, 15–18] that could correspond to hyperenhancement on CT by increasing the volume of distribution of the iodinated contrast agent injected during PCI.

The aim of this study is to evaluate the capabilities of DE-MDCT performed immediately after PCI in predicting the formation of MVO, confirmed by DE-MRI performed a few days later, by studying the density of the myocardium in the infarcted area.

## Materials and methods

### Patient studies

Thirty-four consecutive patients (28 male and 6 female; age range: 38–79 years; mean  $54.3 \pm 11.8$  years) referred to our

institution for a first episode of acute myocardial infarction (MI) between January 2009 and February 2010 were included in the study. MI was diagnosed by the presence of typical chest pain associated with electrocardiogram (ECG) changes, a serum concentration of creatine kinase (CK) of more than twice the upper limit of normal (with more than 5 % of isoenzyme CK-MB) and the presence of an angiographic complete or sub-total occlusion of the infarct-related artery with a TIMI (thrombolysis in myocardial infarction) of 0 or 1 [19]. Inclusion criteria included a TIMI 3 after PCI and the ability to complete a CT examination (Killip I and II [20] with the ability to perform a 15-s breath hold).

All patients underwent CT immediately after PCI and MR within 1 week.

All angioplasty procedures were performed at our institution using iodinated contrast agent (Hexabrix 320 mg/ml, Guerbet, Aulnay-sous-Bois, France) with a mean volume per injection of 10 ml at a rate of 2 ml/s. The total volume of contrast agent used during the revascularisation procedure was recorded.

Informed consent was obtained from all participants after the nature of the procedure had been fully explained. The study was performed in compliance with the requirements of the institutional review board.

### CT imaging protocol

Computed tomography was performed on a Brilliance 64 system (Philips Medical Systems, Best, The Netherlands). Intra-arterial contrast agent was given during the PCI, but no additional contrast agent was given specifically for the CT examination. Patients were transported from the cardiac catheterisation laboratory to the CT equipment as quickly as possible after the PCI. The distance between the two rooms is approximately 50 m. A low-dose, retrospective, ECG-triggered CT of the entire heart was performed using the following parameters: number of detectors 64; individual detector width 0.625 mm; gantry rotation time 420 ms; pitch 0.2; half scan reconstruction mode and cranio-caudal imaging direction. Tube current was fixed to 80 kV and 600 mAs per slice. No ECG tube modulation was used. Reconstruction parameters for axial slices were 2-mm effective section thickness, 1-mm increment, standard intermediate reconstruction filter (kernel CB) and adapted field of view. Retrospective ECG-gated reconstruction in the mid-diastolic phase (75 % of the R-R interval) was performed. A set of three short axis views of the left ventricle were then reconstructed at the base, mid-ventricle and apex using a 7-mm-thick multiplanar reconstruction (MPR) tool (Brilliance Workstation, Philips Medical Systems, Best, The Netherlands) and used for evaluation. The delay between the last contrast agent injection during the PCI and the CT acquisition was recorded.

## MR protocol

Magnetic resonance studies were performed on 1.5-T MRI (Intera, Philips Medical Systems, Best, The Netherlands or Avanto, Siemens, Erlangen, Germany) using a dedicated cardiac coil (five and eight channels respectively). First, ECG-gated, steady-state, free-precession cine images were acquired in the two-chamber, four-chamber and short-axis views. Second, delayed contrast-enhanced MRI was performed after the injection of 0.15 mmol/kg of a gadolinium-based contrast agent (DOTAREM®, Guerbet, Aulnay-sous-Bois, France). A three-dimensional inversion-recovery segmented gradient echo sequence was used in short-axis views. Imaging started 10 min after contrast agent administration, and inversion time was optimised to obtain adequate nulling of the normal myocardial signal (260 to 340 ms). The imaging sequence parameters included an in-plane voxel size of  $1.25 \times 1.25$  to  $1.5 \times 1.5$  mm<sup>2</sup>, slice thickness of 5 mm, flip angle of 25° (Philips) or 10° (Siemens), echo time of 1.4 to 3 ms and repetition time of 4.3 to 9 ms. A set of three short-axis images, matching the anatomical location of the MPR reconstructed CT images, was selected for the analysis. The delay between the CT and MR examinations was recorded.

## Image evaluation

All angiographic images were reviewed by an experienced interventional cardiologist (IS) for TIMI score evaluation before and after reperfusion.

Two experienced observers (CA, LB) evaluated the CT and MR images independently in a random order and blinded to clinical condition and results of the coronarography. For each patient, three CT and three corresponding MR images were analysed. Analysis was performed with in-house dedicated software based on Dicomworks [21]. This software allows CT and MR images to be displayed and the operator to manually draw, on each image, the epicardial and the endocardial contours of the left ventricle. Observers were free to adjust the window width and level values. On each slice, the observer divided the left ventricle into six (for basal and mid-ventricle slices) or four (for apical slices) segments in order to match the 17-segment model [22] described by the AHA. One should note that the 17th segment (corresponding to the apex) was not evaluated with our method. For MRI and CT, each segment was consensually rated as fully assessable (1) or not assessable (0). Finally, the software regularly split each segment into four subsegments in the radial direction of the myocardium using three calculated lines parallel to the epicardial and the endocardial contours (Fig. 1).

For CT images, the mean density of each subsegment was recorded (termed as "absolute density"). Furthermore,

in order to assess the early MVO on CT, sparing of myocardium by contrast enhancement in regions of infarction in the left ventricle (hyperenhanced) was visually rated as present (1) or absent (0).

For MR images, each subsegment was rated as normal, hyper- or hypoenhanced, termed "normal", "infarcted" and "MVO". In the event of disagreement between the two reviewers on MRI classification, a consensual analysis was performed.

Then, in order to normalise the CT values, the relative value of density of each subsegment of a given patient was calculated as the value of the density of the subsegment divided by the mean value of all the "normal" segments for this patient.

Finally, in order to assess total infarct size, infarcted myocardium was delineated on each slice by two observers (LB, BE) and the total volume of infarcted myocardium calculated for MR and CT images.

## Statistical analysis

Values are given as mean  $\pm$  standard deviation (SD). A one-way ANOVA with a clustering by patient and segment method was performed to test the statistical difference in CT absolute and relative density among the three MRI-based groups of subsegments ("normal", "infarcted" and "MVO"). In the event of statistical significance of the global F test, post-hoc Bonferroni tests were computed for comparison between each parameter. A ROC analysis was performed to evaluate the sensitivity and specificity of the relative density on CT to assess the "MVO" subsegments assessed by MRI.

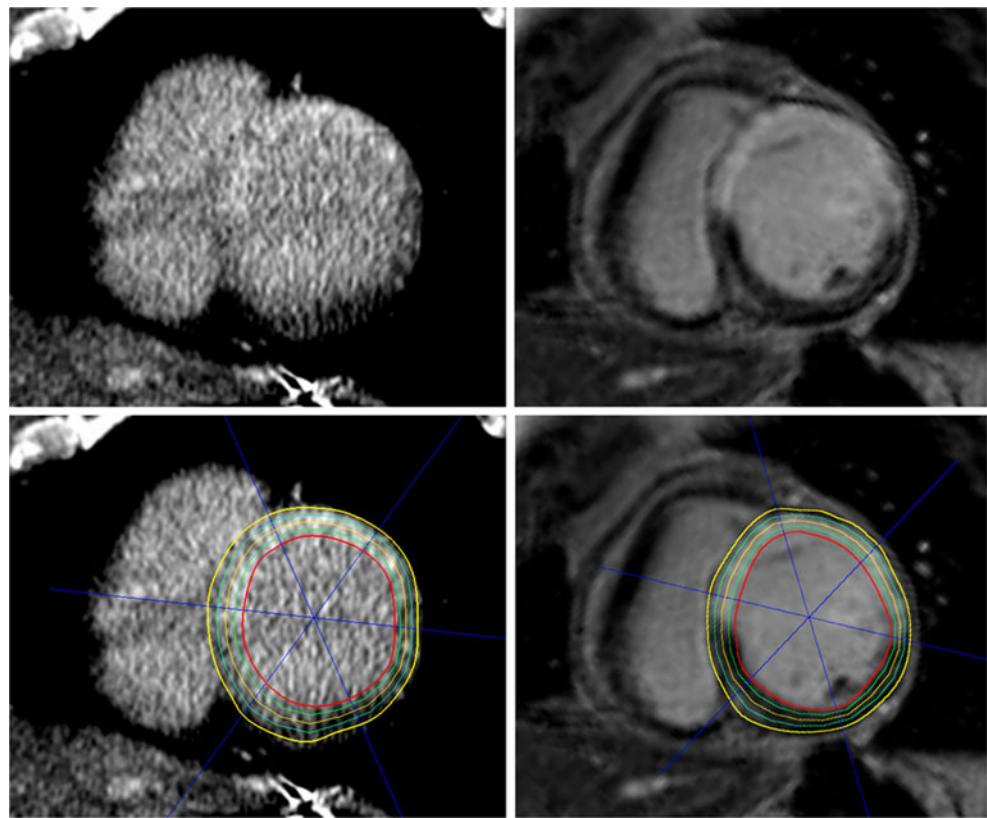
Similarly, the sensitivity and specificity of early MVO on CT in predicting the MRI-assessed MVO subsegments were calculated. One should note that, in order to avoid a regression to the mean, these segments were included in the ANOVA analysis described above.

Correlation between DE-MDCT and DE-MRI for measurement of infarcted myocardium volume was performed using Spearman's rho test.

For each patient the mean absolute CT density was calculated for each group of subsegments. Then a correlation between CT absolute density and total volume of contrast agent injected during the PCI on the one hand and delay between the last contrast agent injection and the CT acquisition on the other hand was performed by using Pearson's correlation coefficient.

To determine the level of inter-reader agreement between the two measurements, the intraclass correlation coefficient (ICC) with its 95 % confidence interval (CI) were calculated for CT and MR measurements. All statistical analysis was performed using Intercooled Stata 10.0 (StataCorp LP, College Station, TX, USA).

**Fig. 1** Delayed enhanced multidetector CT (DE-MDCT; left) and delayed enhanced MRI (DE-MRI; right) in short axis views. Raw images (top) and segmented images (bottom). Epicardial (yellow line) and endocardial (red line) contours are manually drawn. Intermediate lines are then calculated by the software in order to divide the myocardium into four concentric layers. A six- (in this case) or four-branched star (blue) is set to segment the myocardium according to the American Heart Association (AHA) classification



## Results

All 34 of the patients included underwent both the MRI and the CT examination. Two patients were excluded, one because of poor image quality on CT and one because of an incomplete MRI examination (claustrophobia leading to interruption of the examination). Mean delay between the last injection of coronary angiography and the CT was  $19.3 \pm 7.3$  min (range 10 to 45 min). The mean volume of contrast agent injected during the coronary angiography was  $165 \pm 51$  ml (range 40 to 250 ml). MRI was performed  $3.4 \pm 2.5$  days (range 2 to 8 days) after CT.

In the 32 remaining patients, the mean volume of infarcted myocardium was  $24.55 \pm 18.25$  ml (range 0.8–69.6) with DE-MDCT and  $24.1 \pm 17.1$  ml (range 1.8–70.6) with DE-MRI, with a good correlation between the two methods (coefficient of Spearman's  $\rho = 0.96$ ).

Five hundred eight and 500 out of 512 cardiac segments were assessable for CT and MRI respectively. This led to a total of 1,912 subsegments assessable by both MRI and CT. The absolute mean density of CT was  $71.5 \pm 15.8$  HU (range 18.7–144.3 HU),  $103.2 \pm 29.8$  HU (range 42.6–239.5 HU) and  $137.4 \pm 39.8$  HU (range 72.7–251.7 HU) respectively for the MRI-based “normal” (1,421 subsegments), “infarcted” (343 subsegments) and “MVO” (148 subsegments) groups. This led to a significant difference among all three groups

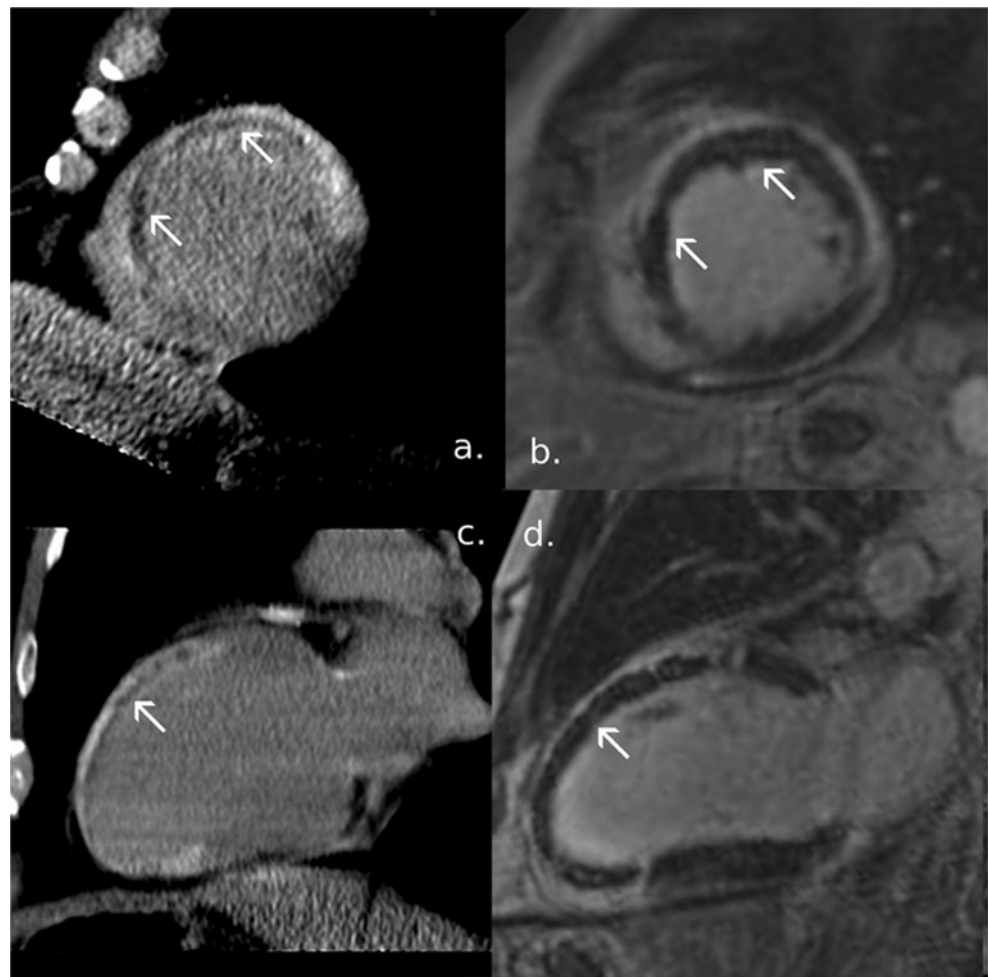
on the ANOVA with post-hoc estimation ( $P < 0.001$ ). Similarly, the mean CT relative density was  $1.0 \pm 0.13$  (range 0.36–1.96),  $1.43 \pm 0.36$  (range 0.65–3.25) and  $1.82 \pm 0.46$  (range 1.0–3.77) for the three groups ( $P < 0.001$ ). Figures 2 and 3 provide a typical example of the data with patients presenting with an MVO assessed by MRI and corresponding to either hypo- (Fig. 2) or hyperenhancement (Fig. 3) on CT. Figure 4 shows an example of a myocardial infarction with an absence of MVO areas on both CT and MRI. Finally, Fig. 5 summarises the mean CT absolute and relative densities for each MRI-based group of subsegments.

Twenty-eight subsegments from 15 segments were represented visually by hypoenhancement on CT. This corresponds to MVO on MRI in 25 subsegments from 14 segments corresponding to a sensitivity and specificity of respectively 16.9 % and 99.8 %. Once these 28 subsegments had been excluded from the ROC analysis, the sensitivity and specificity of the CT relative density for the “MVO” segment were 94.3 % and 89.2 % respectively for a cutoff of 1.36 (corresponding to the mean CT relative density in MVO areas minus 1 SD). Finally, when considering the segment with a relative density of more than 1.36 and the CT hypoenhanced segments, sensitivity and specificity were 95.3 % and 89.3 % respectively.

The correlation between CT absolute density and total volume of contrast agent injected during the PCI was weak,



**Fig. 2** A 57-year-old man with an acute infarction of the anterior wall of the left ventricle. Comparison between DE-MDCT (**a, c**) and DE-MRI (**b, d**) in the short axis (**a, b**) and two-chamber views (**c, d**). In this patient, areas of microvascular obstruction (MVO; arrows) are visualised as hypoenhanced areas with both DE-MDCT and DE-MRI but with a visual underestimation of the MVO extension by CT



with Pearson's correlation coefficients of 0.42, 0.35 and 0.40 for “normal”, “infarcted” and “MVO” areas respectively. Similarly, the Pearson's correlation coefficients were  $-0.1$ ,  $-0.01$  and  $0.0$  for the same group for the comparison between CT absolute density and delay between the last contrast agent injection and the CT image acquisition.

Regarding the inter-reader agreement, the ICC was 0.93 (95 % CI 0.92–0.94) for the CT density analysis, 0.68 (95 % CI 0.65–0.70) for the early MVO on CT analysis and 0.84 (95 % CI 0.82–0.85) for the MR analysis.

## Discussion

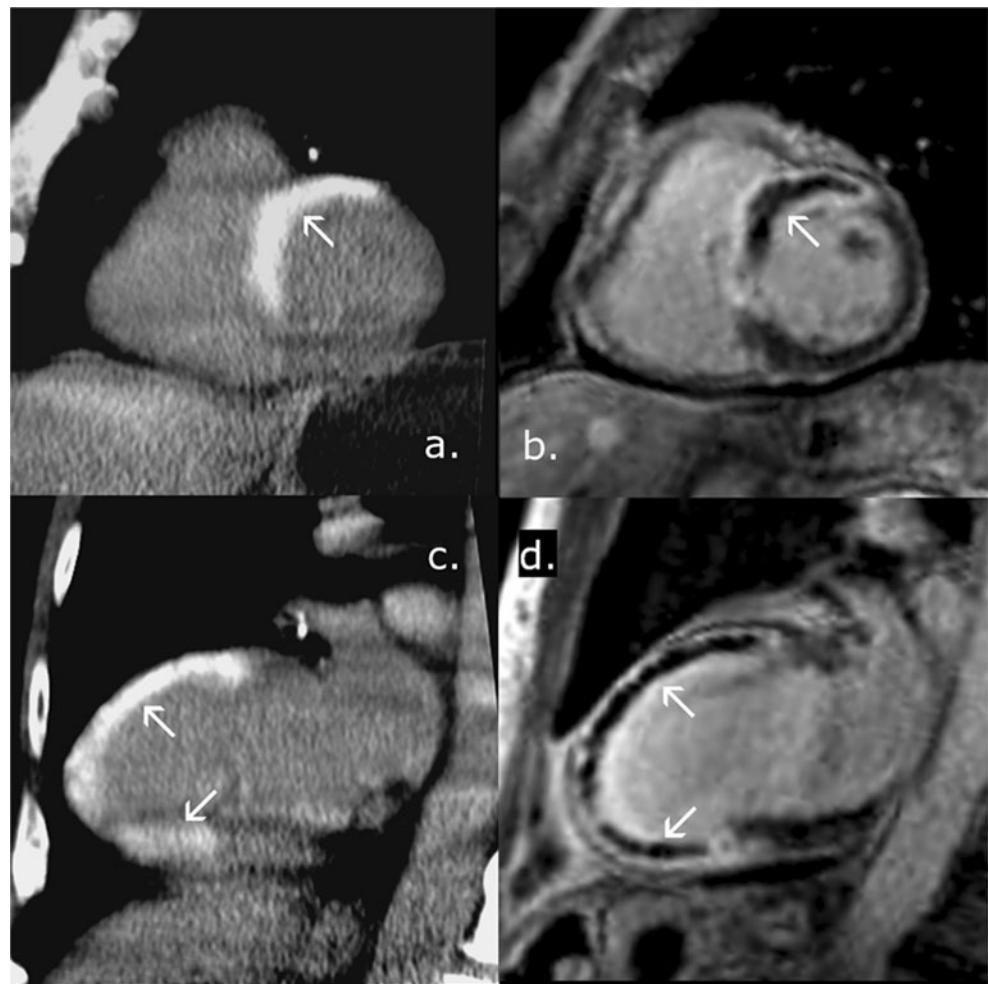
Our study demonstrates that CT, when performed immediately after PCI, can predict the presence of MVO asserted by MRI performed a few days later by studying either the hypoenhancement or the hyperenhancement of the infarcted area. Microvascular obstruction is a complex and dynamic phenomenon corresponding to a lesion of the myocardial microcirculation [6–8, 17] occurring before, during and after the reperfusion [9–11]. In our study, CT was performed

early after recanalisation ( $18 \pm 8$  min) and we probably observed the MVO areas at different stages.

First, CT hypoenhanced areas correspond to early MVO areas with a very high specificity (99.8 %) in comparison with MRI performed a few days later. This aspect of MVO in CT is in accordance with previously published reports [23–25]. Nevertheless, it represents only a small part of the final total amount of MVO (25 out of 148 MVO subsegments in our study). This confirms the underestimation of MVO during the acute phase we previously reported [14].

With regard to the hyperenhanced area on CT the analysis is more complex. When considered globally, the size of these areas closely corresponds to the size of MI measured with MRI as previously demonstrated [13, 14]. But, when considering only the zones with the highest enhancement (more than 1.36 times the normal myocardium), MVO areas can be predicted with a sensitivity of 87.8 % and a specificity of 89.4 %. The physiopathology of this hyperenhancement is complex and outside the scope of our study. Nevertheless, a temporary increase in the blood flow in the “future”

**Fig. 3** A 79-year-old man with an acute infarction of the anterior wall of the left ventricle. Comparison between DE-MDCT (**a, c**) and DE-MRI (**b, d**) in the short axis (**a, b**) and two-chamber views (**c, d**). MVO areas assessed by MRI (arrows) correspond with hyperenhanced areas on CT (mean value of the segments involved of  $1.41 \pm 0.32$  relative to healthy myocardium)



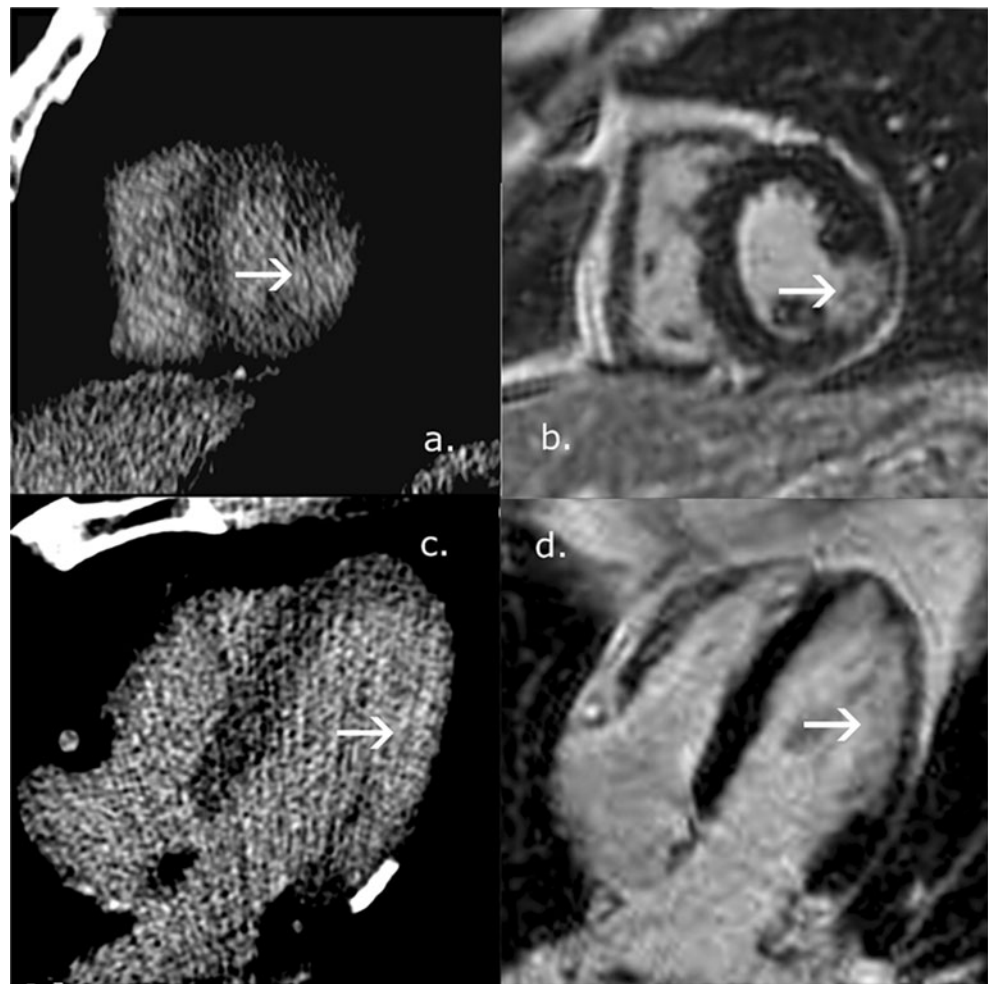
MVO areas certainly plays an important role [6, 17]. Abnormal permeability of endothelium in the future MRI-assessed MVO areas might also increase the ability of contrast material to distribute into the extracellular space of injured myocardium [8]. A lower washout in the more deeply infarcted zone, related to an increase in the distribution volume, and compression of the venous side of the capillary system by the oedema may also be involved [26]. Finally, haemorrhage, which is more likely to be present in the MVO area than in the rest of the infarcted zone [18, 27, 28], may play a role in this increased density.

Finally, considering both these hypo- and hyperenhanced myocardial areas, CT allows the final amount of MVO to be predicted with a good sensitivity and specificity (95.3 % and 89.3 % respectively). This could make CT a good prognostic tool after MI as MVO is an important predictor of adverse outcome in patients such as early post-infarction complications, left adverse ventricular remodelling, recurrent hospital stays for heart failure and mortality [9]. Furthermore, CT can distinguish between MVOs that are already present (hypo-enhanced areas) and incoming MVO (hyperenhanced

area). This element could be useful in distinguishing between the different mechanisms acting in MVO formation: ischaemic injury, distal atherothrombotic embolisation occurring during the angiographic recanalisation and ischaemia-reperfusion injury. Indeed, areas with massive per-PCI microembolism or a long-term related ischaemic lesion might be more likely to present with hypo-enhancement than an ongoing reperfusion lesion. This element could help in evaluating the therapeutic strategies targeting the reperfusion phase such as cyclosporine or post-conditioning [29, 30] by differentiating between the different sources of MVO in patients.

A limitation of this study was the inclusion of only patients presenting with total or subtotal coronary artery obstruction (TIMI 0 or 1 at admission). This increases the proportion of MI with MVO and leads to bias in the sensitivity and specificity calculations. Furthermore the size of our population was relatively small. A larger study including patients with higher TIMI scores will be necessary. Another limitation of our study is the variability of the volume of the contrast agent administered during the PCI and the time between the last

**Fig. 4** A 51-year-old man with an acute infarction of the lateral wall of the left ventricle. Comparison between DE-MDCT (a, c) and DE-MRI (b, d) in the short axis (a, b) and two-chamber views (c, d). In this case, MRI does not show any areas of MVO. The infarcted area appears on CT as a slightly hyperenhanced area with a mean density value relative to healthy myocardium lower than in the case reported in Fig. 3 ( $1.15 \pm 0.07$  versus  $1.41 \pm 0.32$ )



contrast agent injection and CT image acquisition. This is certainly partially responsible for the lack of correlation between CT absolute densities and the volume of contrast agent given and the time between the last injection and image acquisition. However, as this study was performed in the emergency setting, these parameters were not adjustable. We tried to limit this effect by calculating the myocardial densities relative to the healthy myocardium.

In conclusion, when performed immediately after percutaneous coronary intervention, multidetector CT appears as an accurate tool for predicting the final amount of myocardial microvascular obstruction, assessed by MRI performed a few days later, by analysing both the hypo- and hyperenhanced myocardial areas. This could be used as a prognostic tool for acute myocardial infarct outcome but may also be useful in assessing the efficacy of reperfusion lesions targeting therapy.

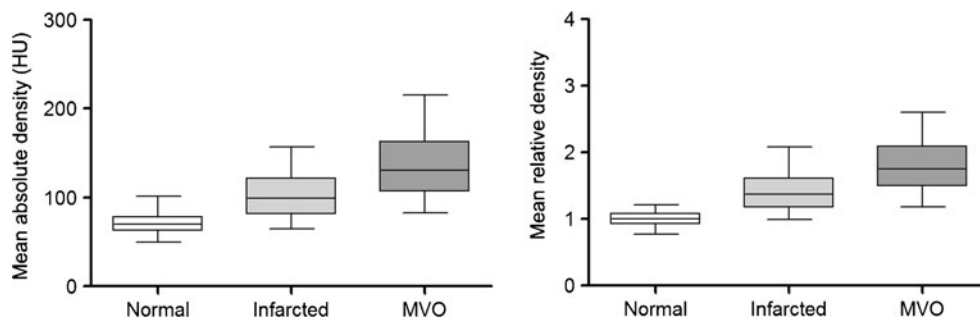


**Fig. 5** Box and whisker plots of mean absolute (left panel) and relative (right panel) CT density for MRI-based normal, infarcted and MVO subsegments. The boxes show the 25th and 75th percentile

(interquartile) ranges. Median values are shown as a horizontal black bar within each box. The whiskers show levels outside the 5th and 95th percentiles

**Acknowledgements** We acknowledge Michel Ovize from the Department of Cardiology, Louis Pradel Hospital, Lyon, France, for his help with this manuscript.

## References

- Bolognese L, Carrabba N, Parodi G et al (2004) Impact of microvascular dysfunction on left ventricular remodeling and long-term clinical outcome after primary coronary angioplasty for acute myocardial infarction. *Circulation* 109:1121–1126
- Brosh D, Assali AR, Mager A et al (2007) Effect of no-reflow during primary percutaneous coronary intervention for acute myocardial infarction on six-month mortality. *Am J Cardiol* 99:442–445
- Cochet AA, Lorgis L, Lalande A et al (2009) Major prognostic impact of persistent microvascular obstruction as assessed by contrast-enhanced cardiac magnetic resonance in reperfused acute myocardial infarction. *Eur Radiol* 19:2117–2126
- Ito H, Tomooka T, Sakai N et al (1992) Lack of myocardial perfusion immediately after successful thrombolysis. A predictor of poor recovery of left ventricular function in anterior myocardial infarction. *Circulation* 85:1699–1705
- Wu KC, Zerhouni EA, Judd RM et al (1998) Prognostic significance of microvascular obstruction by magnetic resonance imaging in patients with acute myocardial infarction. *Circulation* 97:765–772
- Ambrosio G, Weisman HF, Mannisi JA, Becker LC (1989) Progressive impairment of regional myocardial perfusion after initial restoration of postischemic blood flow. *Circulation* 80:1846–1861
- Ito H, Maruyama A, Iwakura K et al (1996) Clinical implications of the 'no reflow' phenomenon. A predictor of complications and left ventricular remodeling in reperfused anterior wall myocardial infarction. *Circulation* 93:223–228
- Kloner RA, Ganote CE, Jennings RB (1974) The "no-reflow" phenomenon after temporary coronary occlusion in the dog. *J Clin Invest* 54:1496–1508
- Niccoli G, Burzotta F, Galiuto L, Crea F (2009) Myocardial no-reflow in humans. *J Am Coll Cardiol* 54:281–292
- Reffelmann T, Kloner RA (2006) The no-reflow phenomenon: a basic mechanism of myocardial ischemia and reperfusion. *Basic Res Cardiol* 101:359–372
- Verma S, Fedak PW, Weisel RD et al (2002) Fundamentals of reperfusion injury for the clinical cardiologist. *Circulation* 105:2332–2336
- Albert TS, Kim RJ, Judd RM (2006) Assessment of no-reflow regions using cardiac MRI. *Basic Res Cardiol* 101:383–390
- Habis M, Capderou A, Ghostine S et al (2007) Acute myocardial infarction early viability assessment by 64-slice computed tomography immediately after coronary angiography: comparison with low-dose dobutamine echocardiography. *J Am Coll Cardiol* 49:1178–1185
- Boussel L, Ribagnac M, Bonnefoy E et al (2008) Assessment of acute myocardial infarction using MDCT after percutaneous coronary intervention: comparison with MRI. *AJR Am J Roentgenol* 191:441–447
- Camilleri JP, Joseph D, Fabiani JN et al (1976) Microcirculatory changes following early reperfusion in experimental myocardial infarction. *Virchows Arch A Pathol Anat Histol* 369:315–333
- Cobb FR, Bache RJ, Rivas F, Greenfield JC Jr (1976) Local effects of acute cellular injury on regional myocardial blood flow. *J Clin Invest* 57:1359–1368
- Rochitte CE, Lima JA, Bluemke DA et al (1998) Magnitude and time course of microvascular obstruction and tissue injury after acute myocardial infarction. *Circulation* 98:1006–1014
- Reffelmann T, Kloner RA (2002) Microvascular reperfusion injury: rapid expansion of anatomic no reflow during reperfusion in the rabbit. *Am J Physiol Heart Circ Physiol* 283:H1099–H1107
- Chesebro JH, Knatterud G, Roberts R et al (1987) Thrombolysis in Myocardial Infarction (TIMI) trial, phase I: a comparison between intravenous tissue plasminogen activator and intravenous streptokinase. Clinical findings through hospital discharge. *Circulation* 76:142–154
- Killip T 3rd, Kimball JT (1967) Treatment of myocardial infarction in a coronary care unit. A two year experience with 250 patients. *Am J Cardiol* 20:457–464
- Puech PA, Boussel L, Belfkih S, Lemaitre L, Douek P, Beuscart R (2007) DicomWorks: software for reviewing DICOM studies and promoting low-cost teleradiology. *J Digit Imaging* 20:122–130
- Cerqueira MD, Weissman NJ, Dilsizian V et al (2002) Standardized myocardial segmentation and nomenclature for tomographic imaging of the heart: a statement for healthcare professionals from the cardiac imaging committee of the council on clinical cardiology of the American heart association. *Circulation* 105:539–542
- Jacquier A, Boussel L, Amabile N et al (2008) Multidetector computed tomography in reperfused acute myocardial infarction. Assessment of infarct size and no-reflow in comparison with cardiac magnetic resonance imaging. *Invest Radiol* 43:773–781
- Lardo AC, Cordeiro MA, Silva C et al (2006) Contrast-enhanced multidetector computed tomography viability imaging after myocardial infarction: characterization of myocyte death, microvascular obstruction, and chronic scar. *Circulation* 113:394–404
- Furtado AD, Carlsson M, Wintermark M, Ordovas K, Saeed M (2008) Identification of residual ischemia, infarction, and microvascular impairment in revascularized myocardial infarction using 64-slice MDCT. *Contrast Media & Molecular Imaging* 3:198–206
- Manciet LH, Poole DC, McDonagh PF, Copeland JG, Mathieu-Costello O (1994) Microvascular compression during myocardial ischemia: mechanistic basis for no-reflow phenomenon. *Am J Physiol* 266:1541–1550
- Basso C, Corbetti F, Silva C et al (2007) Morphologic validation of reperfused hemorrhagic myocardial infarction by cardiovascular magnetic resonance. *Am J Cardiol* 100:1322–1327
- Beek AM, Nijveldt R, van Rossum AC (2010) Intramyocardial hemorrhage and microvascular obstruction after primary percutaneous coronary intervention. *Int J Cardiovasc Imaging* 26:49–55
- Piot C, Croisille P, Staat P et al (2008) Effect of cyclosporine on reperfusion injury in acute myocardial infarction. *N Engl J Med* 359:473–481
- Staat P, Rioufol G, Piot C et al (2005) Postconditioning the human heart. *Circulation* 112:2143–2148